

Exploration of Multiple Wavelength Laser Beams Propagating Underwater

by

Midshipman 1/C Mike Kelly



*A Capstone Project Report Submitted to the Faculty of
The Weapons and Systems Engineering Department
United States Naval Academy, Annapolis, Maryland*

Faculty Advisor: Prof Svetlana Avramov-Zamurovic, Systems Engineering

Department Chair: Prof Brad Bishop

Outside Sponsor: The Office of Naval Research

26APR18

Contents

INTRODUCTION	4
Motivation.....	4
Problem Statement	5
Related Work	5
DESIGN PROCESS	6
Objectives	6
Constraints	6
Functions.....	7
Ethical Considerations	7
Engineering Analysis	8
Component Selection	8
Design Evolution	12
Final Design.....	14
Overview.....	14
Mechanical Setup.....	15
Optical Setup.....	15
Data Collection and Processing	16
Results and Analysis.....	18
Demonstration Plan.....	18
Performance Measures.....	19
Experimental Results	19
Project Management	23
Life Long Learning	23
Cost analysis and Parts List	23
Timeline	24

Discussion and Conclusion 25

Exploration of Multiple Wavelength Laser Beams Propagating Underwater

Author: Midshipman 1/C Mike Kelly

Contact Information: michaeljkelly96@gmail.com, (708) 821 3898

Abstract — Laser beams propagating through complex media commonly experience degradation. This experiment investigates the effects of using laser beams with different wavelengths propagating along the same path as a method of mitigating distortion. We recorded intensity measurements of both a red and green laser after passing through a temperature and flow controlled underwater path and explored the effects of wavelength diversity on laser scintillation. Specifically, temperature variations were induced in a 243cm long water tank, containing 500 liters of deionized water using three heating sources. Experiments were performed with a triple pass through the tank for a total propagation length of 980cm. The final experimentation yielded repeatable and significant reductions in the scintillation of the multiple wavelength beam compared to its individual component beams.

INTRODUCTION

Motivation

With specific reference to communication systems employed by the United States military, laser communication systems stand to offer significant improvements in not only signal transmission security, but the data transfer speed as well. These communication systems could have direct implementation underwater, between divers, submarines, and unmanned underwater vehicles (UUVs). Current undersea communication systems do not frequently rely on wireless systems, particularly when the large transfer of data is imperative to mission success, such as with UUVs, and are slow and unsecure when they do opt for wireless transmission.

Laser link communication systems offer significant improvements over traditional solutions, including increased security and the data transfer speed. Despite these possible advantages, significant barriers in laser propagation have kept the technology from seeing widespread implementation as a means of communication in the US military today. The major challenges facing laser propagation center on overall loss of beam intensity, as well as intensity fluctuations on target over long distances and through different media. In terrestrial environments, there are considerable challenges presented by not only the environmental obscuring effects from airborne particulates, but also the varying of the index of refraction due to temperature gradient changes. These changes affect the beam path and results in constructive and destructive interference upon reception. Similarly, laser beams underwater experience significant challenges in propagation, however there has been significantly less investigation on beam propagation underwater.

Problem Statement

Current research into wavelength diversity has centered on simulation of beams propagating through the atmosphere. This experiment will pass a wavelength diverse laser beam through increasingly turbulent underwater environments to study the effects of wavelength diversity on scintillation when compared to standard Gaussian beams. The experiment will consist of the development of a test bed emulator, which will allow for temperature and turbulence control over the environment. Successful development of the test bed will allow for numerous different environmental permutations, which specifically in this experiment was used to isolate the effects of increased temperature on scintillation, and subsequently look at the differences in scintillation and wavelength diversity.

Related Work

In communications systems, the presence of optical turbulence can have a significant effect on the intensity fluctuations of the beam on the receiver, affecting quality or feasibility of the transmission of data. The underwater environment is particularly susceptible to optical turbulence due to high variability in environmental conditions, such as temperature and salinity. Additionally, the underwater domain is less susceptible to use of high powered lasers due to the possibility of thermal blooming, which occurs when the propagation medium absorbs energy from a propagating beam and is significantly altered in its properties, generally seen as a temperature spike. Because of these issues, both conservation of the beam intensity levels and reduction of scintillation are topics of extreme importance when discussing the feasibility of complex underwater laser systems. Comparatively, there has been markedly less investigation on beam propagation underwater than in the atmosphere, likely due to the difficulty in the set up and control of test beds. This is despite the possible advantages that beam transmissions could bring to the underwater environment, such as advancements in laser communication systems between unmanned underwater vehicles and their control units.¹

One method that has been investigated to cut down on the high degree of intensity fluctuation of laser light on reception, is wavelength diversity². Wavelength diversity involves the use of co-aligned laser beams with diverse wavelengths propagating along the same path onto the same receiver. Existing literature, primarily theory and numerical simulations on wavelength diversity, focuses on propagation through an atmospheric environment³. The theory behind wavelength diversity is based on the way in which laser beams interact with the medium along their propagation path. If two beams have enough wavelength diversity, they will be affected differently and will create inherently different irradiance patterns on the receiver. Where one beam falters, the other beam may be able to fill in, and visa versa. **Figure 1** depicts the received irradiance patterns from a green and red laser influenced by turbulence along the propagation path.

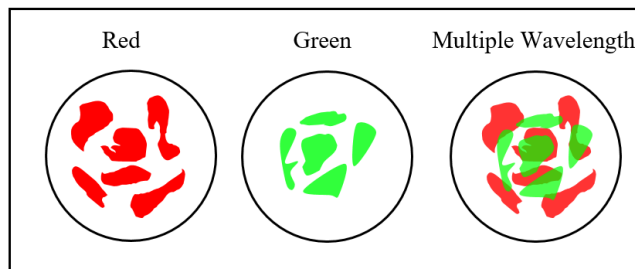


Figure 1. Irradiance Pattern on Receiver for Green/Red/Multiple

Wavelength Beams through turbulence

Much work has also been conducted with focus on underwater LIDAR and mitigation of scattering and backscattering. A lot of the work that has been done experimentally in these experiments can have a good carryover into this experiment. ^{4,5}

There have also been other experiments done in actual ocean scenarios with laser beams. While these experiments do not directly focus on what is being looked at here, they do provide valuable insight into link length, which was something that was going to be experimentally determined. Some of these experiments have led to the belief that the longer the link the more pronounced the effects of optical turbulence, so using a long link would be more beneficial for this experiment. ⁶

DESIGN PROCESS

The test bed emulator was the main focus of the design process. The test bed, a 800 liter polyethylene tank, had to be properly machine cut and have machined windows installed at key points throughout for application to our laboratory set up. This was done first by creating the tank in a three dimensional modeling software, AutoDesk Inventor. After this was done, the preliminary locations for each of the major additions were sent to the machine shop. Work was then conducted in conjunction with the machine shop to develop the final plan, and execute it. After the tank was completed, it was filled with deionized water. The optics set up was then designed and implemented, with several considerations made due to the use of mirrors to create a triple pass system. The overall design did not change much throughout, however the implementation of smaller key features played a bigger role than previously predicted.

Objectives

The main objective of this project was two-fold: to create a controllable test bed emulator to run the tests related to underwater laser propagation, as well as explore the effects of wavelength diversity on beams propagating through turbulent media, specifically looking at temperature and flow, via a laboratory set up which was used to create a beam which would perform in a characteristically similar manner to a multiple wavelength beam.

Constraints

The design space is limited only by the test bed and available laser emitters in the lab. The two laser emitters used were both relatively low power HeNe emitters of differing wavelength. Though it would be possible to perform investigations into wavelength diversity using non-visible light, the two available laser emitters were both in the visible spectrum, and are much more conducive to lab work than non-visible lasers, since alignment is a primary issue. The temperature increments which were used started at room temperature and incremented steadily upward, and the temperature settings were limited by the fact that in the lab we only had heating elements and did not have any cooling elements, which would have enabled temperature ranges below room temperature.

Functions

The test bed would enable a wide variety of environmental scenarios in which a wide variety of optical set ups could test in. Using only the heating sources, the temperatures would range from 70°F to 95°F, controllable to the degree. The heating sources would also create kinetic turbulence, which was used to quantify an even more turbulent environment but also eliminate the bias from the heaters in the turbulence they contributed when analyzing the increased temperatures, which was the initial main focus of the experiment. The mirrors within the tank would be set up in such a way that, confirming with trigonometry, there would be capability for at least a triple pass system, with potential for even longer path lengths. **Table 1** showcases the desired functions of the system in environmental modeling, and the highlighted portion is what was used. This experiment was conducted under highly ideal conditions, however the tank has the ability to accommodate much more complex environments.

	Minimum	Initial Testing with Experimental Setup	Extensive Testing with Experimental Setup
Temperature	Minimum Control over temperature (2 experimentally distinct settings)	Control over temperature above room temperature (10+ experimentally distinct temp settings)	Control above and below room temperature (20+ experimentally distinct temp settings)
Flow	2 experimentally distinct flow settings (self-contained)	Free manipulation of flow power (self-contained)	Free manipulation of flow power (reservoir)
Turbidity	No Requirement	Addition of 1 particulate matter	Addition of numerous types of particulate matter
Salinity	No Requirement	No Requirement	Control over salinity

This testbed apparatus leaves a lot of room for further environmental permutations which could be used to further develop testing procedures. This experiment focused on the addition of heat and flow into the tank in a very simple manner.

Ethical Considerations

The only ethical considerations that need to be made concern the wildlife that live within the propagation medium. Regarding underwater laser propagation, this consideration is made for fish and other wildlife that

inhabit the sea state in which the lasers would be propagated. Laser beams are scattered as they propagate through water, which can affect the optic nerves of animals if the light scatters into the eyes of the wild animals. Though this may not be a concern strictly for this experiment, the real world application for the work done in this experiment carries with it ethical considerations which affect a number of different forms of wildlife, and in a real world scenario, should be considered.

Engineering Analysis

There were a number of important assumptions which were used, mainly regarding test environment constraints and other control variables. Much of the engineering analysis done on this system was conducted in the design portion for the test bed, and not during the actual experimentation. Engineering analysis was conducted mostly using AutoDesk Inventor, a desktop manufacturing design tool. The test bed was created in this software, and initial modification specifications were drawn out and converted into engineering drawings, all described in further detail below.

There was no computer modeling software which could have been used to predict temperature flow distribution or laser interaction with the environment, at least not within the scope of this experiment.

Component Selection

-Experimental Test Bed

The experimental test bed to be used in this experiment is 243x76x43cm, giving it a total volume capacity of 800 liters. It is made of polyethylene. For practical application to the experiment, the TSD Machine Shop helped make several adjustments to the tank. Holes were cut into the top and sides, to be used as access ports and viewports, respectively. Metal rings 20cm in diameter were also machined to be fitted around the acrylic used as viewports, sandwiching optical acrylic between them and forming a window, as pictured below in **Figure 2**.



Figure 2. Metal Retaining Ring with Window

Roof access ports were also installed. Each of these access ports are covered in a marine quality deck plate fitting, measuring 20cm across at the middle (**Fig 3**).



Figure 3. Roof Deck Plate Fitting

The windows are machined metal rings sandwiching optical quality acrylic from AcryLite. The windows (**Fig 4**) measure 10cm in diameter. The decision was made to put them lower on the height of the tank so that the experiments can be conducted in the tank without requiring to fill the tank more than half way, which still totals several hundred pounds of water. The windows will be able to hold the weight of the water up to the filled capacity of the tank, however unlikely such a scenario may be.



Figure 4. Entry and Exit Viewports

-AquaScape AquaSurge 2000 Adjustable Flow Pump

This experiment initially requires a pump to fill up the tank, however, the pump could also be used in later iterations of the experiment to create flow inside the tank. The pump (**Fig 5**) that has been purchased for

this experiment is classically used in outdoor ponds. It has a very high output speed, capable of filling the test bed in a matter of minutes. At a total output of ~7570 liter/hr, this pump is more powerful than needed for the experiment, as well as for use in more advanced systems, such as a system with flow capabilities. Fortunately, this pump has a controllable output which is controlled by the wireless remote (Fig 6).



Figure 5. AquaScape AquaSurge 2000



Figure 6. Controller

This will allow for a number of faster and slower speeds, which will ultimately be imperative for the future addition of flow into the system, however this is not currently a consideration for the test bed.

-ThorLabs Kinematic Pitch and Yaw Mount

The mounts which actually held the lasers were 2 degree of freedom kinematic mounts, which allowed for manipulation of the pitch and yaw of the laser, which was highly important for this experiment since the alignment of the lasers was of such critical importance. **Figure 7** shows the pitch and yaw mount.



Figure 7. ThorLabs Kinematic Pitch and Yaw Mount

-ThorLabs XYR1 Rotational Mount

One of the more useful items which was used in this experiment was the XYR laser mounts (**Figure 8**). These mounts are called XYR due to the axes of manipulation they allow for the user. They include two axes of movement linearly (X, Y), as well as a rotational element (R). The alignment of the beams is always a difficult task, but coupling the Pitch-Yaw laser mounts on top of these mounts will increase control to a 5 degree of freedom system, with lateral up and down movement being the only uncontrolled aspect of the set up. These mounts, pictured below, made the alignment of the multi-laser system much faster and allow for minute tweaks to the locations of the beam spots, which will result in better data collection, particularly after a long propagation path such as the one used in this experiment.



Figure 8. ThorLabs XYR Mount

-REO R-33361 Green HeNe Laser

The green visible laser used in this experiment was from REO. It is a 2mW beam at 543 nm wavelength (visible green). **Figure 9** shows this laser with its control source.



Figure 9. REO Green HeNe laser emitter

-ThorLabs HNL020L Red HeNe Laser

The red visible laser used in this experiment was from ThorLabs. It is a 2mW beam at 632.6 nm wavelength (visible red). **Figure 10** shows this laser with its control source.



Figure 10. ThorLabs Red HeNe laser emitter

-ThorLabs 340M-GE CCD Camera

For data collection, a CCD camera, also from ThorLabs, was utilized. It was able to collect data quite quickly, approximately 55 frames/second, and with an exposure time of 17ms. These were the experimental collection parameters that were utilized for every data collection. Neutral Density filters had to be applied to attenuate the light to avoid saturation of the sensitive receiver. **Figure 11** shows the CCD Camera.



Figure 11. ThorLabs CCD Camera

Design Evolution

The design evolved steadily over time due to the unpredicted requirements from the use of large volumes of water, functionality of the heating elements, and manipulability of the optical set up. In the initial engineering drawings of the tank and the modifications required, pictured below in **Figure 12**, the initial plan was to have two roof access points, spaced equidistant from each other and the two side walls.

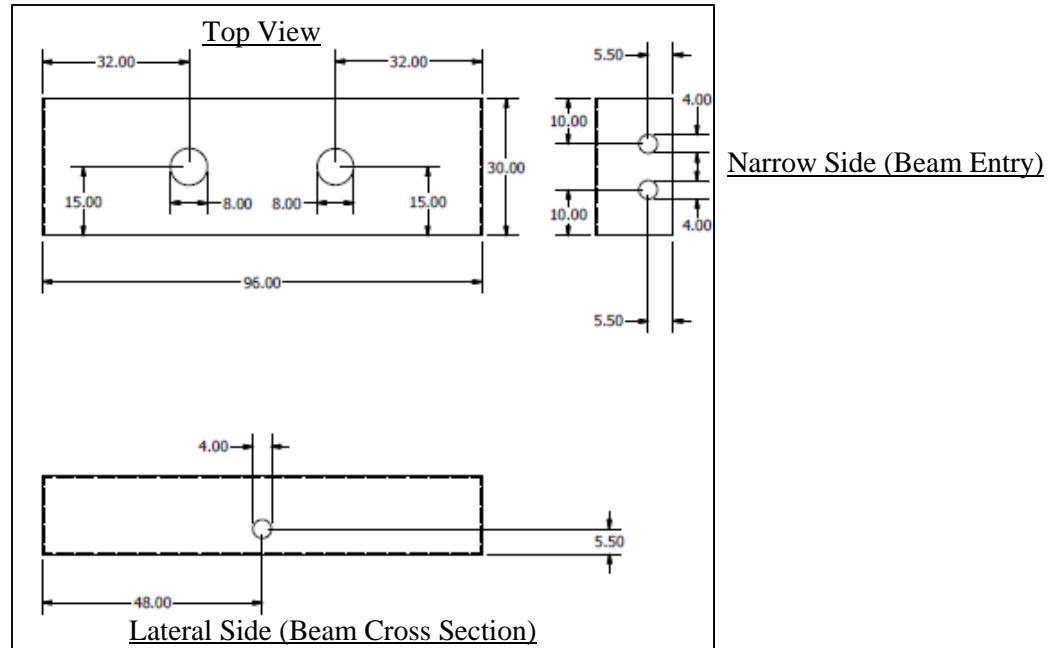


Figure 12. Initial Engineering Drawing of Tank including dimensioned cuts

This design was overturned and redrawn in the machine shop with the eventual realization that the roof holes were too far away from the two edge pieces to get into the tank and set up the mirrors and to finish the machine work on the two beam entry and exit windows. The solution to this problem was to expand to three roof access points, with two heaters 45cm in from the sides and another directly in the middle. This allowed for manual manipulation of the mirrors inside the tank, while also giving us three points to put the heaters into the water.

The initial design also included the construction of a suspension bridge between the roof access points, which would function as a mounting rail for the heating elements. This bridge would have to be assembled inside the tank using modular pieces. These pieces were printed using additive manufacturing in the Gamma Lab in Maury. Each piece consisted of a male and female end of two styles which press fit into each other. Each was 1 foot long, and made of ABS plastic. There were additional mounting pieces which were dropped down into the roof access points which acted as the anchors for these bridge pieces. While in the design phase this worked, in practice the heaters were too tall to properly function in every portion of the tank, since they expelled water out of the bottom, and if that flow was too close to the bottom of the tank it would result in increased and unpredictable turbulence. The solution to this issue was to convert the drop-in anchor points to become the new heater suspenders. While this took away from the overall functionality of the tank since the heaters were no longer able to be placed anywhere along the central axis, as was initially the plan, this change was ultimately a good change for this experiment, since the temperature increases were frequent, and access the control panel on the heaters would have been much reduced if they were spread throughout the closed tank. The drop in support is pictured below in **Figure 13**.



Figure 13. Drop in Heater Mount with heater

Final Design

Overview

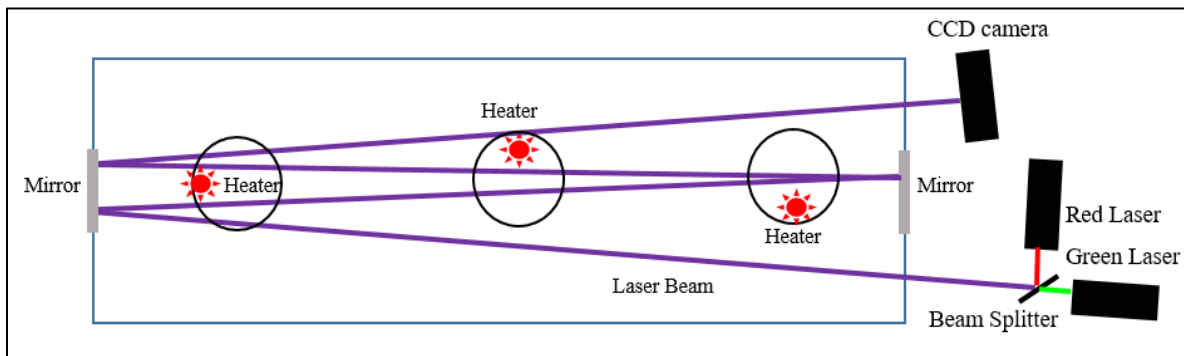


Figure 14. Overhead lab setup

Figure 14 depicts an overhead view of the laboratory set up, from the optics to the tank and then to the data collection system. The only part of the experimental setup which is not included was the data processing unit, which for this experiment was a laptop running MatLab. Each of the three major subsystems (mechanical, optical, data processing) are detailed below. Begin with a functional block diagram and a picture of your completed design. At the least, present the mechanical, electrical and software sub-systems as shown below. Consider making additional subsections to present other subsystems.

Mechanical Setup

The bulk of the mechanics within this experiment came from the design of the tank, and mostly included things that interacted with the water, like the heaters. The heaters used in this experiment were spaced along the medial axis of the tank, 45cm from the edges of the tank and another 76cm from each heater at the exact middle of the tank. **Figure 15** shows the dimensions of the tank as it appeared in the lab.

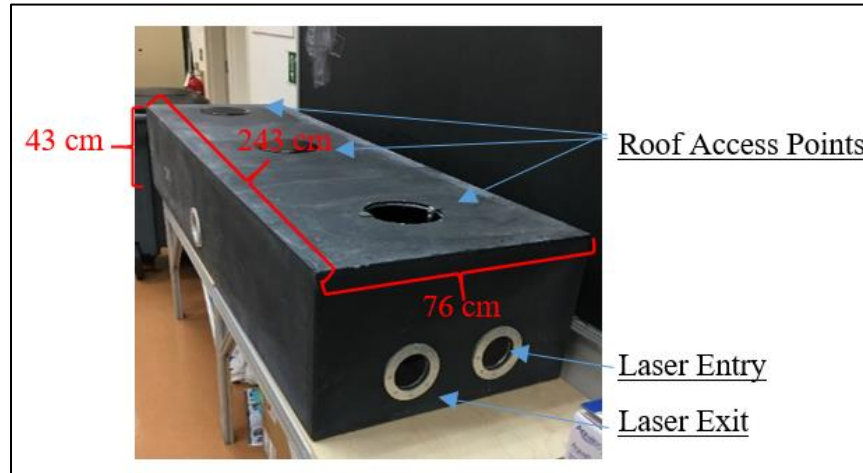


Figure 15. Experimental Test Bed with Dimensions in Lab

Optical Setup

The other major item in the experimental setup was the optics set up. The optics had to be positioned in such a way as to mimic the effects experimentally of a wavelength diverse laser beam. To do this, light was emitted from two laser sources of different wavelengths and projected into a beam splitter (basically a mirror with 50% reflectance/50% transmittance), which combines the beams onto the same path. For the purposes of this experiment, the light was considered to be on the same beam path if the entry and exit points in the tank were the same, both of which could be confirmed by using the camera to check for intensity peaks for both beams at both of those locations.

The laser emitters were mounted in specifically designed laser holders, which were bolted into a screw board. These mounts were actually two different mounts which had been combined, with one secured to the top of the other. The result was a 5 degree of freedom manually controlled system, with pitch, yaw, rotational angle, and x- and y- displacement all controlled by the operator. This allowed effectively any beam path to be used, and allowed easy manipulation of the other laser so that the beam paths lined up.

For data collection, a Charge Coupled Device Camera (CCD) was used to collect the data. It was mounted on the same peg board, with manual manipulation of its rotational angle as well as x-/y- displacement and height. This camera was outfitted with neutral density filters to dilute the power of the light as it was received by the camera, since the unfiltered light would easily saturate the sensitive sensors in the camera. The attenuation power of the neutral density filters was experimentally determined to yield the best mathematical calculations, since the actual power received by the camera was not something that affected the statistical measures of intensity fluctuation.

The optics setup is show below in **Figure 16**.

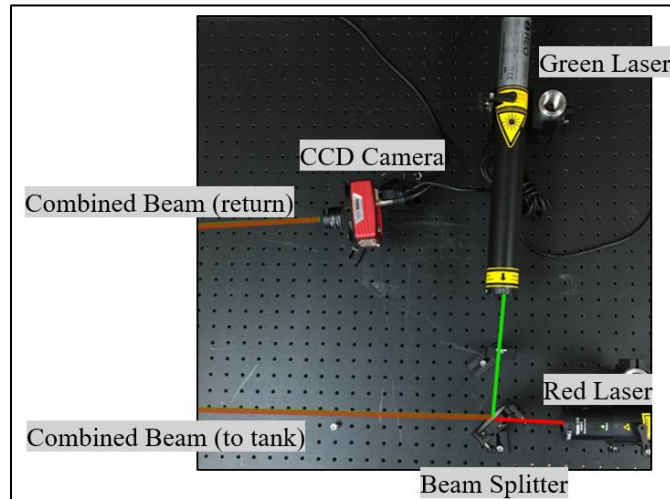


Figure 16. This is an overhead view of the optical setup, with the most important pieces each labeled.

Data Collection and Processing

Laser light intensity fluctuations were recorded by the sensor on the CCD camera. Data was downloaded onto a laptop computer as a series of .tif screens, which were each analyzed individually. In each pixel of the 480x640 resolution screen captures, intensity fluctuation were recorded. The background intensity value for the CCD camera was determined experimentally, and was subtracted from the values. From these, the scintillation was calculated as a statistical measure as the normalized variance of the intensity fluctuations. These were then averaged across the beam profile as an average for each pixel throughout the collection. Pixels with a mean irradiance value greater than or equal to $\frac{1}{e^2} * Max Intensity$ were considered within the beam profile as per the traditional definition of the spot size of a laser beam. This helped particularly to avoid the issues with intensity fluctuation spikes at the edge of the beam profile due to low saturation, and also created what is called a masked beam profile. **Figures 17** and **18** are two angles of an ideal result of masked beam intensity profile.

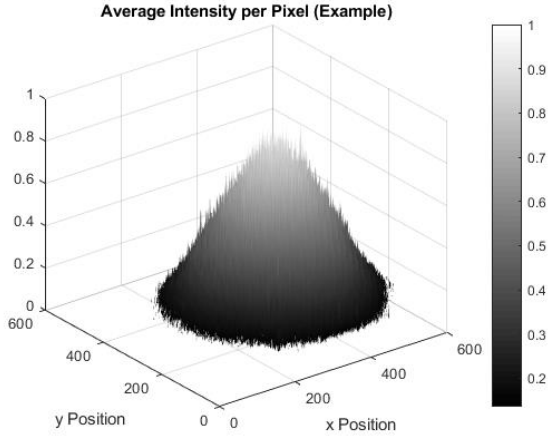


Figure 17. Beam Profile Side View

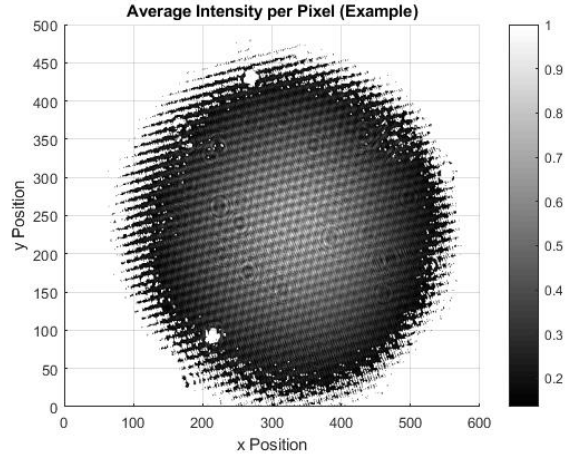


Figure 18. Beam Profile Receiver Planar View

The scintillation index of a beam is the resulting normalized variance of irradiance fluctuations. The normalized variance is computed for a laser beam upon arrival at the receiver, and this value effectively describes the frequency of irradiance fluctuations. Below is the equation for the calculation of scintillation index, denoted as SI and where I is the irradiance of the optical wave and I_{avg} is the average irradiance on that particular screen

$$SI = \frac{(\langle I^2 \rangle - \langle I_{avg} \rangle^2)}{(\langle I_{avg} \rangle^2)} \quad (1)$$

This unit-less value is determined from the readings by the camera at the end of the tank receiving the beam. The normalized variance, or scintillation index, can be computed as a statistical value for beams of all powers and spot sizes, allowing the value to be compared across a wide array of beam types and sizes. In doing so, scintillation index was used to compare the performance of the beam intensity fluctuations for all beams used in this experiment.

The heat sources had to be placed in such a way that they were in a very close proximity to the beam path. This ultimately resulted in a large amount of turbulence being generated around each of the heater, shown in **Figure 14** as the red circular objects with traces coming off. To account for this and to try and track the impact that the temperature alone was having on the propagation performance, two data collections were conducted at each temperature interval. The “agitated” collection was done with the heating element turned on, and after it had reached a steady state heat output. The “calm” collection was conducted after the water had ample time to settle with the heater turned off, which was standardized at a 5 minute interval. **Figures 19** and **20** showcase the typical beam profile for each of these cases.

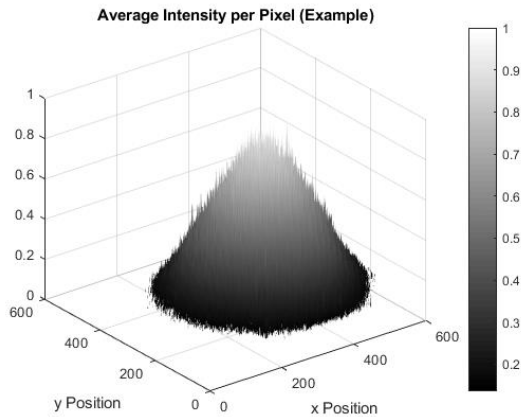


Figure 19. Calm Tank Green Beam Profile (70°F)

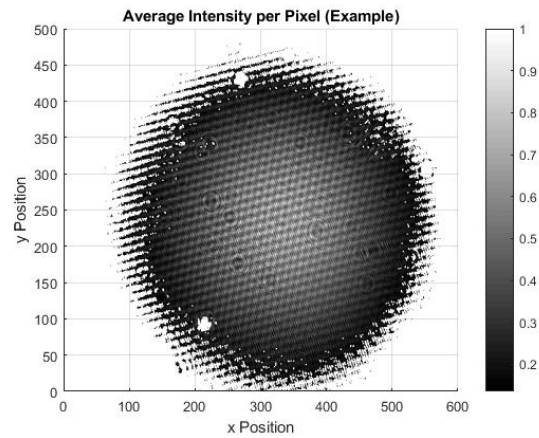


Figure 20. Agitated Tank Green Beam Profile (70°F)

The MatLab code itself, included in **Appendix A**, was modified from code initially developed for tests such as these, but only for use with one single beam and data point. The final code that was developed for this project ran all three data collections at each temperature and turbulence at once, so that the values could be properly compared. **Figure 21** shows pseudo-code for the analytics code used in this experiment.

```

Read in Red Beam Screens

    Calculate First Moment (Average Intensity) for all
    Pixels

    Calculate Second Moment (Scintillation) for all
    Pixels

    Mask Beam by calculating beam spot parameters

    Plot Masked and Unmasked Versions for this Beam

Repeat Process for Green Beam

Repeat Process for Combined Beam

Compare Resultant Values and Output Data

```

Figure 21. Pseudo-code for MatLab data processing algorithm.

Results and Analysis

Demonstration Plan

To conduct the experiment, the water was first brought from room temperature (~67°F) to 70°F and allowed to stabilize at this temperature. After there was no more fluctuation in the temperature readings

off of the heating elements, the beams, which had been left on for several minutes before hand to stabilize, were aligned along the same beam path onto the receiver. The data was then collected for the green beam, then the red beam, and finally the combined beam. After the data was collected, the beams were left on and the heaters were all turned off for a period of 5 minutes. After that calming time had elapsed, the data was collected again in the same manner. After the “calm” data was collected at that temperature, the temperature was incremented another 5°F. This process was repeated from 70°F to 95°F, and always in the same order. While the temperatures would increase, the data was run through the processing algorithm to check for high variability. Rarely, if ever, was there a bad data collection. The collections were for a period of approximately 12 seconds, in which 600 screens were procured at a rate of ~55 frames/second and an exposure time of 17ms. Ultimately, the most time consuming process of the experiment was waiting for the water to heat up, but once it did, it was able to maintain that heat for long periods of time due to the mass of the water.

Performance Measures

The performance of the test bed was quantified by the degree of manipulation of the test bed, as well as the consistency and repeatability of the results. The experiment was conducted a total of 4 times, with similar trends and data values being observed each time. The results in the graphs below, used in the paper for SPIE, were the most recent and also the cleanest results, which is why they were displayed. The fact that the mean variance calculations for each of the successive tests were on par with each other validated the data collection and processing methods for that portion of the experiment, which is arguably the most important and certainly the most computationally intensive.

The test bed was supposed to be able to step accurately the temperature up 5°F for each temperature setting, and be able to stabilize at that temperature without any widespread fluctuation. This functionality was accomplished. Though the initial desire was to have some type of controllable flow, the testbed design was not conducive to including that in this experiment, so instead, we used the characteristics of actuators (the heaters) that had already been implemented into the system. As mentioned above, the creation of the “calm” and “agitated” environmental states helped isolate the bias from the kinetic turbulence in the water without bringing in any other testing apparatus which would have only served to further complicate the experiment.

Experimental Results

Because the theory of multiple wavelength propagation improving scintillation performance has to do with minute changes in the index of refraction over the beam propagation path, as well as the effect as a function of wavelength, it is very much possible that too short a path length would not result in scintillation reduction. The beam path was increased by more than 500% in the second experiment, and the results were much more conclusive.

Table 2 shows in detail the results of the data collection at each of the temperature settings, with distinction between the agitated and calm environmental settings. Scintillation calculated as a unit-less value, and intensity is stored as a measure of charge recorded from the receiver, which uses the incident photons to create a measurable electrical charge.

Scintillation						
	70F	75F	80F	85F	90F	95F
Red Calm	0.0078	0.1088	0.2926	0.3754	0.3113	0.6336
Standard Deviation	0.0076	0.0835	0.1762	0.1723	0.1676	0.3492
Green Calm	0.0616	0.1175	0.2900	0.5690	0.4916	0.9937
Standard Deviation	0.0868	0.0926	0.1798	0.2660	0.1795	0.4491
Both Calm	0.0004	0.0984	0.2467	0.2434	0.4333	0.5533
Standard Deviation	0.0003	0.0920	0.1482	0.1329	0.1767	0.2766
Red Agitated	0.0089	0.0667	0.2919	0.7014	0.7526	0.8299
Standard Deviation	0.0115	0.0511	0.1127	0.1295	0.2163	0.1821
Green Agitated	0.0165	0.1045	0.3322	0.8291	0.8370	1.5024
Standard Deviation	0.0189	0.1249	0.1361	0.1975	0.1462	0.3824
Both Agitated	0.0107	0.0663	0.2388	0.5822	0.3972	0.8096
Standard Deviation	0.0127	0.0739	0.0993	0.1337	0.1199	0.2520
Intensity						
	70F	75F	80F	85F	90F	95F
Red Calm	899.3565	777.1502	664.6414	685.7734	822.8711	472.4281
Standard Deviation	310.53	294.09	261.02	185.56	194.71	183.12
Green Calm	2865.8602	2122.7952	2180.5239	1380.1393	1481.1217	937.2033
Standard Deviation	1113.70	878.32	751.41	479.79	476.96	362.71
Both Calm	3417.2260	2873.2188	2540.6331	2685.0828	2331.2792	1226.2385
Standard Deviation	1281.90	1065.90	1010.45	683.40	722.27	394.59
Red Agitated	962.4209	914.9258	724.9596	685.4959	378.1893	512.4732
Standard Deviation	304.06	292.07	258.98	258.87	109.94	103.29
Green Agitated	2442.0617	1993.8349	1725.8987	1549.5102	1628.3403	905.2385
Standard Deviation	996.82	790.70	711.85	473.14	483.78	406.57
Both Agitated	2899.5192	2380.9301	2303.2392	2067.5316	2320.7106	1626.5954
Standard Deviation	1004.94	925.79	850.49	816.39	943.50	516.77

Table 2. Scintillation and Intensity Data from Experimentation.

The data from the table is compiled in the following Figures (22, 23, 24, 25), displaying scintillation or intensity vs temperature for both calm and agitated data.

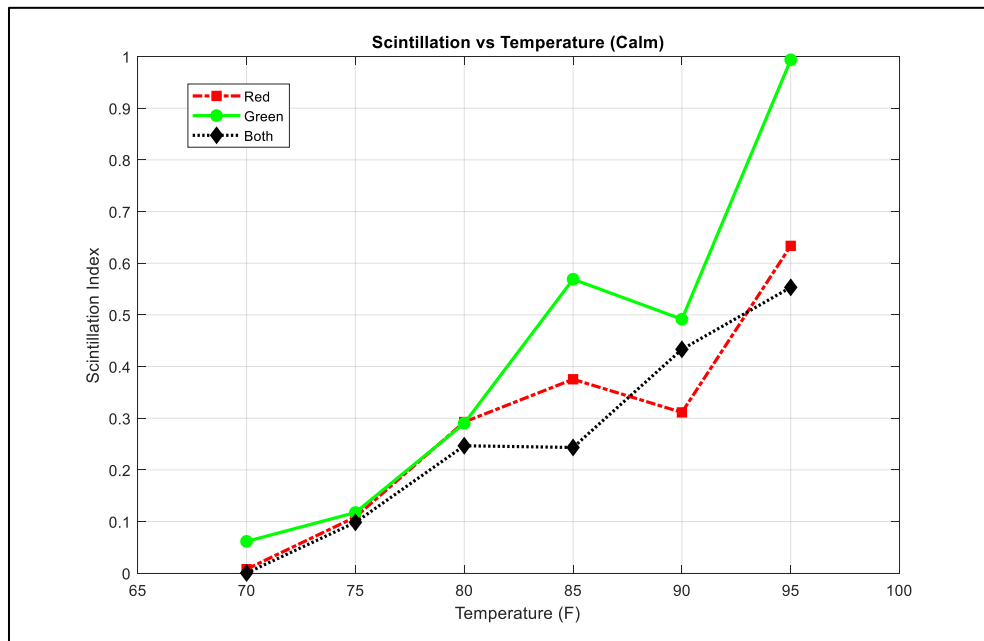


Figure 22. Scintillation vs Temperature (Calm)

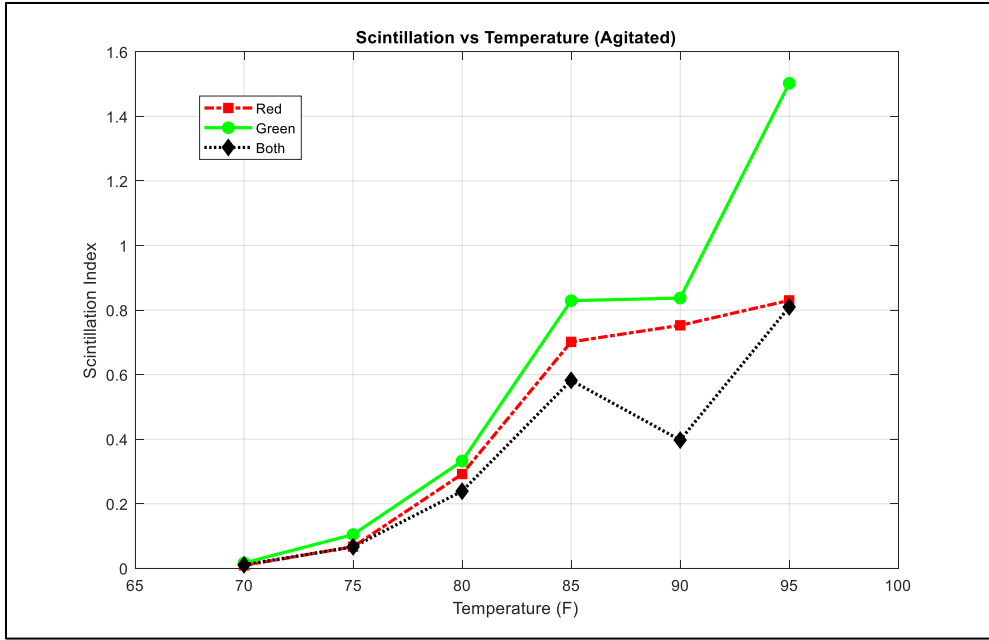


Figure 23. Scintillation vs Temperature (Agitated)

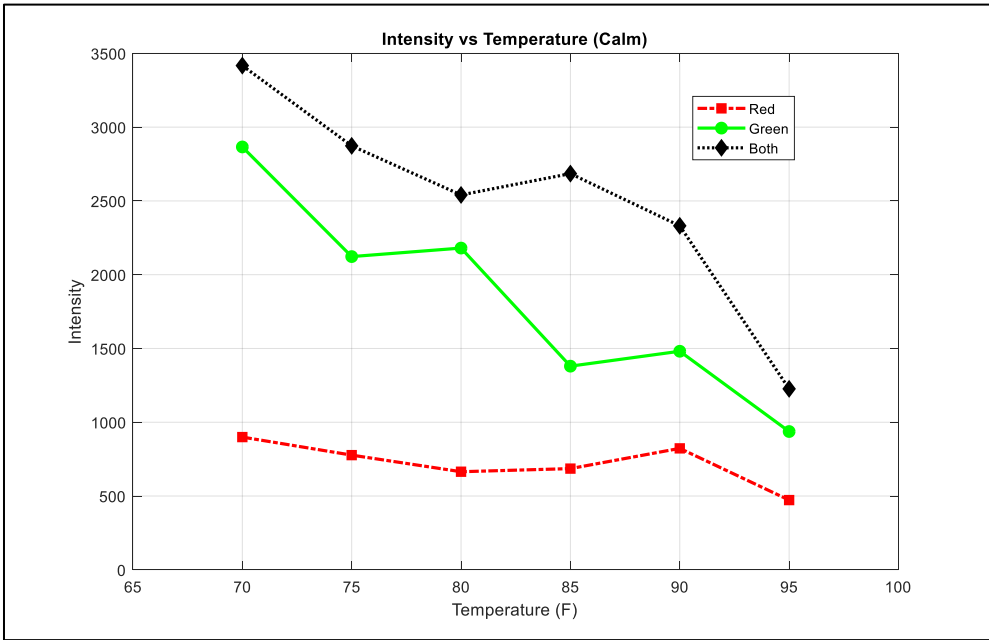


Figure 24. Intensity vs Temperature (Calm)

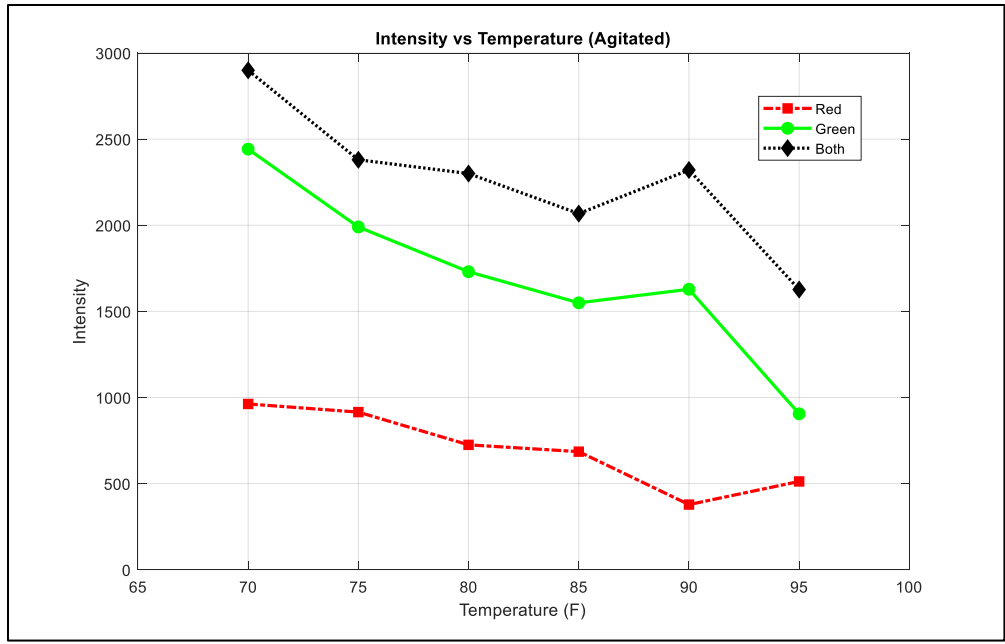


Figure 25. Intensity vs Temperature (Agitated)

The data analysis shows clear trend lines. Most notably, the multiple wavelength beam consistently outperformed the other beams with respect to scintillation reduction, with the exception of one temperature setting. For the agitated environment, there was an overall average reduction in scintillation by 27.77%, while the calm environments yielded an average reduction of 31.05%. At almost every temperature increment, the green beam performed the worst, despite markedly less absorption as it propagated through the environment when compared to the red beam.

Additionally, the beams all performed comparatively worse as the temperature increased in both calm and agitated conditions, demonstrating the theory about increased optical turbulence as the temperature of the system increased. The effects of temperature increase on the beams overall reduced the intensity while increasing the scintillation, providing a much worse environment for something such as communications.

These values and deductions come with a caveat due to the high value of the standard deviation calculated along with them. Due to the high degree of beam spread and turbulence, it was repeatedly a difficult process to keep the beam centered on the receiver on the camera, and as such, the resulting standard deviations are higher than desired. If possible, mitigation of these affects would provide more comprehensive data, however every effort was made to keep the beam centered as it got progressively more turbulent as the experimentation went on. Each of these collections were repeated multiple times under identical experimental set ups to test the repeatability of measurements, since even minute changes to the heater placement or beam orientation from collection to collection would result in discernable changes.

Project Management

Life Long Learning

This project's contribution to my own learning has been two fold. For one, I have learned what it takes and what it means to truly conduct research. I had not before had any exposure to this branch of science to such a degree. My research experience culminated with a trip to an actual academic conference in which I presented and defended my work. I learned a lot about the development of the research process as well. Unfortunately, it is not as simple as actually just doing a laboratory experiment and talking about what you did. It expands well beyond that, and the frustrations and the successes will contribute to how I think critically about things in the future.

Additionally, I learned an extensive amount about the laser technology that was being studied, including laser communication systems and real world applications for systems such as directed energy weapons. Many systems are being developed and implemented for use in the Navy for a number of different applications. As an officer, it is highly important to have a strong foundational understanding of the science behind complicated technological systems, and this process has given me that insight for this field.

Cost analysis and Parts List

Part	Quantity	Cost/Unit	Total Cost
95 Gallon Trash Can	1	239.95	239.95
Tubing	1	36.95	36.95
XYR1 Laser Mounting Stage	2	639.54	1279.08
LMR1 Lens Mount	2	15.23	30.46
BSN16 Beamsplitter	1	192.78	192.78
Utility Broadband Mirror	2	102.00	204.00
Optical Plexiglas*	1	58.58	58.58
AquaSurge Pro Pump*	1	439.99	439.99

Beckson Marine Deck Plate*	2	34.99	69.98
210 Gal Poly Tank*	1	689.99	689.99
Parts (total)			3241.76
Labor (hr) (lab + shop)	200	15	3000.00
Total			6241.76

* - Denotes something that was purchased in support of this project in the Spring '17.

Table 3. Part Cost Analysis Table

The overall cost of the project including labor was approximately 6200\$, with much of that value coming from the specific and highly precise laser mounting tools, the cost of the tank itself, as well as the labor that went into the construction of this test bed on behalf of both our team and the team in the machine shop, who worked on the tank, including the fitting of the windows, for several days.

Timeline*

1. Fall Semester
 - a. Weeks 1-16: Equipment purchasing and prototyping for tank (Since Spring '17 saw completion of pre-Capstone work early)
2. Spring Semester
 - a. Weeks 1-6: Additional Equipment Purchasing and Test Bed Assembly
 - i. Acrylic Window Construction
 - ii. Machine Shop Work Coordinated
 - b. Weeks 6-12: Optical Setup, Tank Filling, and Initial Experimentation
 - i. Distilled water from USNA Chem lab
 - ii. Optics apparatuses either ordered or appropriated from other laser lab work
 - iii. Data Collection in fully functional tank
 - c. Weeks 12-End: Data Analysis, Capstone Finalization, SPIE Conference
 - i. Data analysis (3x recollection as well)
 - ii. Poster/Paper finished for Capstone
 - iii. Attended SPIE Ocean Sensing and Monitoring X as poster session presenter in Orlando, FL.

* - Gantt chart developed in earlier classes was no longer valid since it was developed with hope for Trident acceptance

Discussion and Conclusion

Current laser communication systems have not yet been refined enough for feasible application in the underwater domain. Possible advances in the understanding of laser types which could be more conducive to underwater propagation, such as multiple wavelength beams, could make underwater laser communication possible in the future. Advances must focus on not only the preservation of laser intensity, so as to travel longer distances, but also on the minimization of intensity fluctuations, which are detrimental to the success of a communications system.

This paper explored the performance of a red-green multiple wavelength beam in a series of scenarios, and compared the performance of this beam to the performance of its component beams. The motivation for the experimentation comes from the theory that laser beams with different wavelengths will interact with changes in refractive index along the propagation path differently, which could ensure higher and more sustained saturation of the receiver compared to a beam of a single wavelength. Ultimately, this experiment has yielded the intended result as an investigation of the effects of propagation of multiple wavelength laser beams in the underwater environment. A second, larger tank was used to refine the experiment since the beam needed a longer propagation path in the environment, often with more kinetic turbulence in the environment as well. As temperature increased, the amount of scintillation and overall reduction in intensity also increased. The reduction in scintillation caused by the use of the multiple wavelength beam, however, was constant across all of the experimental environments and conditions. The combined beam was consistently slightly higher intensity than the sum of the other two beams, which also supports that more of the light was hitting the receiver than if either beam had been propagated on its own.

While the experiment has proven useful, there are a number of new issues raised from the developments that have been made. Looking for ways to reduce the standard deviation of measurements would be important to finding more and more meaningful data. Further experimentation into the effects of temperature gradients which change linearly would be valuable, and the addition of particulate matter in the tank to act as “scatterers” would be an interesting next step. Additionally, looking at the effects of two beams that are further away on the EM spectrum would also be valuable in helping to determine the true effects of wavelength diversity and the possible advantages it may have.

From a systems design perspective, the test bed design was realized in the final product, and a successful test of lasers in the water was carried out. In that test, work that had never yet been done in the field was conducted, and a positive result came about from it. Ideally, there would be a way to exert more control over the temperature and kinetic turbulence independently, which was impossible in this scenario because the heaters were in fact causing the kinetic turbulence, however the results from this experiment did a satisfactory job in the isolation of the temperature and the effects from the water agitation. It is also highly infeasible to heat the entire tank to a certain temperature without introducing some type of kinetic mixing, since it would take an extremely long time for the temperature to diffuse away from the heat sources and mix more evenly throughout the tank.

Acknowledgments

I would like to specifically thank Professor Avramov-Zamurovic for all of the work she has done with me from plebe year academic counseling through capstone consultation. Additionally, Professor Charles Nelson has been a great help and encouragement along the way. This project could not have happened without the expertise and assistance provided by the Technical Support Division of the Weapons and Systems Department, as well as the Multimedia Support Center. Funding was provided by the Office of Naval Research. Additional support came from the Research Office at the Naval Academy.

References

- [1] B. Cochenour, D. Alley, L. Mullen, "Mobilizing optical underwater imaging and communications", PowerPoint, NAVAIR Laser/Magnetics Advanced Technology Branch Patuxent River, MD.
- [2] Trinh-Thi-Kim Tran, Øyvind Svensen, Xuyuan Chen, and Muhammad Nadeem Akram, "Speckle reduction in laser projection displays through angle and wavelength diversity," *Appl. Opt.* 55, 1267-1274 (2016)
- [3] Robert Purvinskis, Dirk Giggenbach, Hennes Henniger, Nicolas Perlot, Florian David, "Multiple-wavelength free-space laser communications", *Proc. SPIE 4975, Free-Space Laser Communication Technologies XV*, (3 July 2003); doi: 10.1117/12.478932; <http://dx.doi.org/10.1117/12.478932>
- [4] L. Mullen, S. O'Connor, B. Cochenour, F. Dagleish, "State-of-the-art tools for next-generation underwater optical imaging systems", PowerPoint, Harbor Branch Oceanographic Institute, Ocean Visibility and Optics Lab, Fort Pierce, FL.
- [5] B. Cochenour, D. Alley, L. Mullen, "Mobilizing optical underwater imaging and communications", PowerPoint, NAVAIR Laser/Magnetics Advanced Technology Branch Patuxent River, MD.
- [6] G. Nootz, E. Jarosz, F. R. Dagleish, and W. Hou, "Quantification of optical turbulence in the ocean and its effects on beam propagation," *Appl. Opt.* 55, 8813-8820 (2016)

Appendix A: MatLab Code

```
format long e
format compact
name1=['both.tif'];
FileTif=name1;
InfoImage=imfinfo(FileTif); mImage=InfoImage(1).Width;
nImage=InfoImage(1).Height;NumberImages=length(InfoImage);
FinalImage=zeros(nImage,mImage,NumberImages,'uint16');
firstmom=zeros(nImage,mImage); secondmom=zeros(nImage,mImage);
sil=zeros(nImage,mImage); z=1;
ax=1; bx=NumberImages;
for i=ax:bx
    FinalImage(:,:,z)=imread(FileTif,'Index',i);b=double(FinalImage(:,:,z));
    firstmom=firstmom+b; secondmom=secondmom+(b).^2;
a(z)=b(200,200);z=z+1;ab(z)=mean(mean(b));
end
```

First calc

```
todiv=NumberImages;

firstmom= firstmom/todiv;secondmom= secondmom/todiv;
```

Average Intensity/Pixel

```
firstmom_nonatt = firstmom;

firstmom_max_both = max(max(firstmom_nonatt));

Global_firstmom_max = firstmom_max_both;

firstmom_normalized = (firstmom_nonatt/Global_firstmom_max);
```

Both X Maxes

```
for i=1:1:numel(firstmom_normalized(1,:))
    both_int_y_maxes(i) = max(firstmom_normalized(:,i));
end
```

Both Y Maxes

```
for i=1:1:numel(firstmom_normalized(:,1))
    both_int_x_maxes(i) = max(firstmom_normalized(i, :));
end
```

Scintillation

```
si=secondmom./(firstmom).^2-1;
```

SI Average Within Beam

```
v1=si(:);stdsi=std(v1);

v2=firstmom(:);stdavg=std(v2);

int_logic = v2 > (1/exp(2))*firstmom_max_both;

logic_v1 = int_logic .* v1;

v1_trunc = logic_v1(logic_v1 ~= 0);

si_mean_beam_both = mean(v1_trunc)
```

Cut the SI

```
logic_int = firstmom > 1/exp(2)*firstmom_max_both;

si_coordinates = logic_int .* si;

zeros_si_coord = si_coordinates;

si_coordinates(si_coordinates == 0) = NaN;
```

Average Intensity Within Beam

```
logic_v2 = int_logic .* v2;
```

```
v2_trunc = logic_v2(logic_v2 ~=0);

beam_spot_avg_int_both = mean(v2_trunc);
```

Normalized Average Intensity Within Beam

```
logic_v21 = int_logic .* firstmom_normalized(:);

v21_trunc = logic_v21(logic_v21 ~=0);

beam_spot_avg_int_both_norm = mean(v21_trunc);
```

Cut the Int

```
int_coordinates = logic_int .* firstmom;

int_coordinates(int_coordinates == 0) = NaN;
```

Plotting

SI - Zeros

```
figure(12);surf(zeros_si_coord);shading interp; colormap Hot; title(['DiChromatic
Scintillation = ' num2str(si_mean_beam_both)]); xlabel('x Position'); ylabel('y
Position');
% SI - new method
figure(1);surf(si_coordinates);shading interp; colormap Hot; title(['DiChromatic
Scintillation = ' num2str(si_mean_beam_both)]); xlabel('x Position'); ylabel('y
Position');
% Intensity - new method
figure(2);surf(int_coordinates); shading interp; colormap Hot; title(['Combined Beam
Only Average Intensity per Pixel = ' num2str(beam_spot_avg_int_both) ' (Not
normalized)']); xlabel('x Position'); ylabel('y Position');
% Original Intensity
figure(5);surf(firstmom_normalized); shading interp; colormap Hot; zlim([0 1]);
title(['Combined Beam Intensity per Pixel = ' num2str(beam_spot_avg_int_both_norm) '
(Normalized)']); xlabel('x Position'); ylabel('y Position');
clear si firstmom secondmom
name1=['green.tif'];
FileTif=name1;
InfoImage=imfinfo(FileTif); mImage=InfoImage(1).Width;
nImage=InfoImage(1).Height;NumberImages=length(InfoImage);
FinalImage=zeros(nImage,mImage,NumberImages,'uint16');
firstmom=zeros(nImage,mImage); secondmom=zeros(nImage,mImage);
```

```

sil=zeros(nImage,mImage);z=1;
ax=1;bx=NumberImages;
for i=ax:bx
    FinalImage(:,:,z)=imread(FileTif,'Index',i);b=double(FinalImage(:,:,z));
    firstmom=firstmom+b; secondmom=secondmom+(b).^2;
a(z)=b(200,200);z=z+1;ab(z)=mean(mean(b));
end

```

First calc

```

todiv=NumberImages;

firstmom= firstmom/todiv;secondmom= secondmom/todiv;

```

Average Intensity/Pixel

```

firstmom_nonatt = firstmom;

firstmom_max_green = max(max(firstmom_nonatt));

firstmom_normalized = (firstmom_nonatt/Global_firstmom_max);

```

Both X Maxes

```

for i=1:1:numel(firstmom_normalized(1,:))
    green_int_y_maxes(i) = max(firstmom_normalized(:,i));
end

```

Both Y Maxes

```

for i=1:1:numel(firstmom_normalized(:,1))
    green_int_x_maxes(i) = max(firstmom_normalized(i, :));
end

```

Scintillation

```

si=secondmom./(firstmom).^2-1;

```

SI Average Within Beam

```

v1=si(:);stdsi=std(v1);

v2=firstmom(:);stdavg=std(v2);

```

```
int_logic = v2 > (1/exp(2))*firstmom_max_green;

logic_v1 = int_logic .* v1;

v1_trunc = logic_v1(logic_v1 ~= 0);

si_mean_beam_green = mean(v1_trunc)
```

Cut the SI

```
logic_int = firstmom > 1/exp(2)*firstmom_max_green;

si_coordinates = logic_int .* si;

zeros_si_coord = si_coordinates;

si_coordinates(si_coordinates == 0) = NaN;
```

Average Intensity Within Beam

```
logic_v2 = int_logic .* v2;

v2_trunc = logic_v2(logic_v2 ~=0);

beam_spot_avg_int_green = mean(v2_trunc);
```

Normalized Average Intensity Within Beam

```
logic_v21 = int_logic .* firstmom_normalized(:);

v21_trunc = logic_v21(logic_v21 ~=0);

beam_spot_avg_int_green_norm = mean(v21_trunc);
```

Cut the Int

```
int_coordinates = logic_int .* firstmom;

int_coordinates(int_coordinates == 0) = NaN;
```

Plotting

SI - Zeros

```
figure(13);surf(zeros_si_coord);shading interp; colormap Hot; title(['Green
Scintillation = ' num2str(si_mean_beam_green)]); xlabel('x Position'); ylabel('y
Position');
% SI - new method
figure(6);surf(si_coordinates);shading interp; colormap Hot; title(['Green
Scintillation = ' num2str(si_mean_beam_green)]); xlabel('x Position'); ylabel('y
Position');
% Intensity - new method
figure(7);surf(int_coordinates); shading interp; colormap Hot; title(['Green Beam Only
Average Intensity per Pixel = ' num2str(beam_spot_avg_int_green) ' (Not normalized)']);
xlabel('x Position'); ylabel('y Position');
% Original Intensity
figure(8);surf(firstmom_normalized); shading interp; colormap Hot; zlim([0 1]);
title(['Green Beam Intensity per Pixel = ' num2str(beam_spot_avg_int_green_norm) '
(Normalized)']); xlabel('x Position'); ylabel('y Position');
clear si firstmom secondmom
name1=['red.tif'];
FileTif=name1;
InfoImage=iminfo(FileTif); mImage=InfoImage(1).Width;
nImage=InfoImage(1).Height;NumberImages=length(InfoImage);
FinalImage=zeros(nImage,mImage,NumberImages,'uint16');
firstmom=zeros(nImage,mImage); secondmom=zeros(nImage,mImage);
sil=zeros(nImage,mImage); z=1;
ax=1;bx=NumberImages;
for i=ax:bx
    FinalImage(:,:,z)=imread(FileTif,'Index',i);b=double(FinalImage(:,:,z));
    firstmom=firstmom+b; secondmom=secondmom+(b).^2;
a(z)=b(200,200); z=z+1; ab(z)=mean(mean(b));
end
```

First calc

```
todiv=NumberImages;

firstmom= firstmom/todiv;secondmom= secondmom/todiv;
```

Average Intensity/Pixel

```
firstmom_nonatt = firstmom;

firstmom_max_red = max(max(firstmom_nonatt));
```

```
firstmom_normalized = (firstmom_nonatt/Global_firstmom_max);
```

Both X Maxes

```
for i=1:1:numel(firstmom_normalized(1,:))
    red_int_y_maxes(i) = max(firstmom_normalized(:,i));
end
```

Both Y Maxes

```
for i=1:1:numel(firstmom_normalized(:,1))
    red_int_x_maxes(i) = max(firstmom_normalized(i, :));
end
```

Scintillation

```
si=secondmom./(firstmom).^2-1;
```

SI Average Within Beam

```
v1=si(:);stdsi=std(v1);

v2=firstmom(:);stdavg=std(v2);

int_logic = v2 > (1/exp(2))*firstmom_max_red;

logic_v1 = int_logic .* v1;

v1_trunc = logic_v1(logic_v1 ~= 0);

si_mean_beam_red = mean(v1_trunc)
```

Cut the SI

```
logic_int = firstmom > 1/exp(2)*firstmom_max_red;

si_coordinates = logic_int .* si;

zeros_si_coord = si_coordinates;

si_coordinates(si_coordinates == 0) = NaN;
```

Average Intensity Within Beam

```
logic_v2 = int_logic .* v2;

v2_trunc = logic_v2(logic_v2 ~=0);

beam_spot_avg_int_red = mean(v2_trunc);
```

Normalized Average Intensity Within Beam

```
logic_v21 = int_logic .* firstmom_normalized(:);

v21_trunc = logic_v21(logic_v21 ~=0);

beam_spot_avg_int_red_norm = mean(v21_trunc);
```

Cut the Int

```
int_coordinates = logic_int .* firstmom;

int_coordinates(int_coordinates == 0) = NaN;
```

Plotting

SI - Zeros

```
figure(14);surf(zeros_si_coord);shading interp; colormap Hot; title(['Red
Scintillation = ' num2str(si_mean_beam_red)]); xlabel('x Position'); ylabel('y
Position');
% SI - new method
figure(9);surf(si_coordinates);shading interp; colormap Hot; title(['Red Scintillation
= ' num2str(si_mean_beam_red)]); xlabel('x Position'); ylabel('y Position');
% Intensity - new method
figure(10);surf(int_coordinates); shading interp; colormap Hot; title(['Red Beam Only
Average Intensity per Pixel = ' num2str(beam_spot_avg_int_red) ' (not normalized)']);
xlabel('x Position'); ylabel('y Position');
% Original Intensity
figure(11);surf(firstmom_normalized); shading interp; colormap Hot; zlim([0 1]);
title(['Red Beam Intensity per Pixel = ' num2str(beam_spot_avg_int_red_norm) '
(Normalized)']); xlabel('x Position'); ylabel('y Position');
figure(3); hold on; plot(both_int_x_maxes, 'm');plot(green_int_x_maxes, 'g');
plot(red_int_x_maxes, 'r'); title('X Intensity'); xlabel('X Position');
ylabel('Intensity');ylim([0 1]);legend('Combined', 'Green', 'Both');
% Comparison (y)
```

```
figure(4); hold on; plot(both_int_y_maxes, 'm');plot(green_int_y_maxes, 'g');  
plot(red_int_y_maxes, 'r'); title('X Intensity'); xlabel('X Position');  
ylabel('Intensity');ylim([0 1]);legend('Combined', 'Green', 'Both');
```